Molecular Dynamics Study of Polymer−Water Interaction in Hydrogels. 2. Hydrogen-Bond Dynamics

Yoshinori Tamai* and Hideki Tanaka

Department of Polymer Chemistry, Graduate School of Engineering, Kyoto University, Kyoto 606-01, Japan

Koichiro Nakanishi

Department of Chemical Technology, Kurashiki University of Science and the Arts, Nishinoura 2640, Tsurajima-cho, Kurashiki, Okayama 712, Japan

Received July 1, 1996[⊗]

ABSTRACT: Molecular dynamics simulations have been performed for hydrogel models of poly(vinyl alcohol) (PVA), poly(vinyl methyl ether) (PVME), and poly(*N*-isopropylacrylamide) (PNiPAM). The dynamics of hydrogen bonds and the translational and rotational motions of water molecules in the vicinity of the polymer segments are analyzed to investigate the properties of water molecules which are highly cooperative with the surrounding polymer chains. The characters of the hydrophilic groups which are reflected in the lifetime of hydrogen bonds, the spectral density, etc., are examined. The mobility of water molecules is significantly lowered around polymer chains for both translational and rotational motions. This is partly because of the hydrogen bonds between water and polymers around the hydrophilic groups and partly because of the structuralization of water around the hydrophobic groups.

Introduction

In the hydrogels, which are made of hydrophilic polymer and water, structure and stability of water molecules are highly perturbed by polymer matrices, as elucidated in our previous paper[1] through molecular dynamics (MD) simulation for hydrogel models of poly(vinyl alcohol) (PVA), poly(vinyl methyl ether) (PVME), and poly(*N*-isopropylacrylamide) (PNiPAM). Polar groups in the polymers strongly bind water molecules and yield defects in water−water hydrogen bonds in the vicinity of the groups. The hydrogels simulated contain also nonpolar groups, which cause so-called hydrophobic effects in the solvated structure of the polymers. Water−water hydrogen bonds are enhanced and stabilized around hydrophobic groups especially for PVME and PNiPAM, which have large hydrophobic groups in side chains.

The mobility of water molecules in hydrogels is significantly depressed by slowly relaxing polymer matrices. Destruction and re-formation to hydrogen-bond networks are necessary for water molecules to diffuse. The dynamics of hydrogen bonds is expected to contribute to the various time-dependent phenomena in hydrogels. As reviewed by Ladanyi and Skaf,[2] single-particle and hydrogen-bond dynamics has been studied for hydrogen-bonding liquids: water, methanol, aqueous solutions of small molecules, etc. Collective motion and fluctuation of hydrogen-bond networks in liquid water have also been studied as reviewed by Ohmine and Tanaka.[3] These studies on water and small molecules will also serve to elucidate the dynamics of hydrogels.

In the previous paper[1] (hereafter called Part 1), equilibrium results and structure and stability of hydrogen-bond networks are presented for the hydrogel models of PVA, PVME, and PNiPAM with various water contents under several temperature conditions. In the present article, the dynamics of hydrogen bonds is analyzed, using trajectories of MD simulations obtained in Part 1. The translational and rotational motions of water are investigated and related to the hydrogen-bond dynamics and to the equilibrium solvation structures.

Model and Simulation Details

In this article, all the analyses are performed using the trajectory files which are obtained in Part 1.[1] The initial configurations of hydrogel models of poly(vinyl alcohol) (PVA), poly(vinyl methyl ether) (PVME), and poly(*N*-isopropylacrylamide) (PNiPAM) are obtained by the procedure presented in Part 1. Water contents are 0, 25, 50, 75, and 100 wt %. MD simulations are performed under *NPT* ensemble[4,5] at a pressure of 0.1 MPa at five temperatures (400, 350, 300, 250, 200 K). The AMBER/OPLS[6] force field is used for the polymers, and the SPC/E[7] for water. The united atom approximation is applied for $-CH_3$, $-CH_2-$, and $>CH-$ groups, each of which is treated as a single interaction site. The long-range Coulombic interactions are handled by the Ewald sum method.[8] The short-range Lennard-Jones terms of the potentials are cut off at 9 Å, and the long-range correction terms are added. The bond angles, H−O−H of water and CH−O−H of PVA, and all the bond lengths are constrained by the SHAKE algorithm.[9] The total sampling time amounts to 50 ps (100 000 steps) at each temperature. A detailed description of the simulation is given in Part 1.[1]

All the dynamical quantities and time correlations are calculated from the 5000 configurations saved by 0.01 ps interval and are averaged over all the time origins t_0. Water dynamics are analyzed in three classified regions: (1) those around hydrophilic groups, (2) those around hydrophobic groups, and (3) the bulk region. The classification is based on the polymer−water radial distribution functions as described in Part 1.[1]

Results and Discussion

Residence Rate of Water. The water molecules diffuse from one region to another with the passage of time. The residence rate, $P_{res}(t)$, is defined as the probability that the water molecule which exists in one region at time t_0 stays in the same region at later time $t + t_0$, not departing from the region. $P_{res}(t)$ is averaged

[⊗] Abstract published in *Advance ACS Abstracts,* September 1, 1996.

S0024-9297(96)00961-8 CCC: $12.00

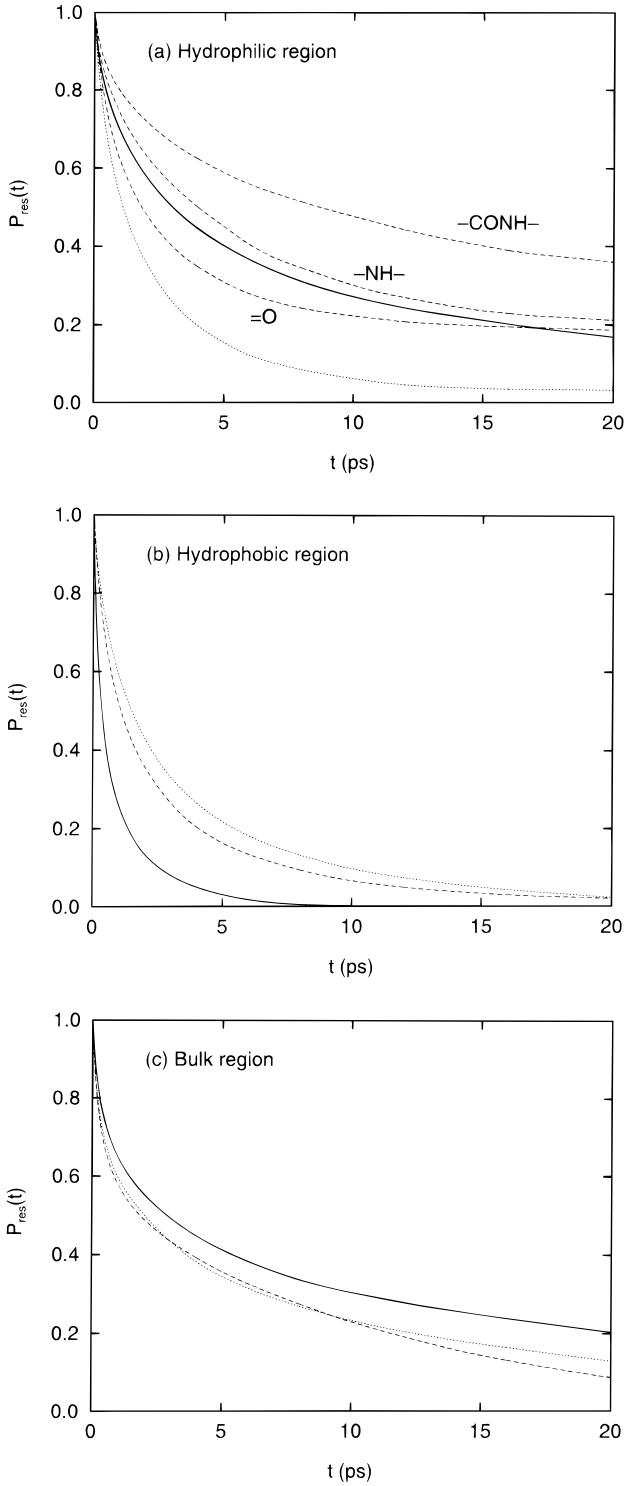

Figure 1. Residence rate $P_{res}(t)$ of water at 300 K for (a) hydrophilic region, (b) hydrophobic region, and (c) bulk region: (solid line) PVA, (dotted line) PVME, (dashed line) PNiPAM.

over all the time origins t_0 of 0.01 ps interval. Figures 1a, 1b, and 1c show $P_{res}(t)$ at 300 K for the hydrophilic, hydrophobic, and bulk regions, respectively. The decay curves of $P_{res}(t)$ is understandable in terms of polarity of polymers (see Table 2 of Part 1) and size of the region (see Table 6 of Part 1).

In the hydrophilic region $P_{res}(t)$ have long tails because the hydrogen bonds between water and polymers bind the water molecules to the region for a long time. For PVA $P_{res}(t)$ decays slowly since PVA has highly polar sites and the hydrophilic region spreads continuously. For PVME $P_{res}(t)$ decays fast since −O− of PVME is less polar than −OH of PVA and the average cluster volume of the region is small.

For PNiPAM $P_{res}(t)$ decays slower than as expected from polarity and cluster volume of the region. Although −NH− group is less polar and has much smaller cluster volume around the group than that around −OH group, $P_{res}(t)$ of −NH− resides for a longer time than that of −OH. Although the partial charges and cluster volumes are the same for −O− and =O, $P_{res}(t)$ of =O resides for a longer time than that of −O−. The reason for these observations is that the groups =O and −NH− of PNiPAM are located in a somewhat isolated space from the bulk solvent; water molecules around the groups are hard to leave the area. Since the region around −CONH−, which includes those around both =O and −NH−, is a combined wide space for water molecules to move around, $P_{res}(t)$ resides for a much longer time period.

In the hydrophobic region, $P_{res}(t)$ decreases faster than that in the hydrophilic region because the hydrophobic groups form no hydrogen bonds with water. For PVME and PNiPAM, the relaxations of $P_{res}(t)$ are slower than those for PVA because the volumes of the hydrophobic region are large (see Table 6 of Part 1) for former two polymers and also mobility of water is decreased by the structuralization of water molecules around $-CH_3$ groups. For PVME, the relaxation of $P_{res}(t)$ in the hydrophobic region is the same rate as that in the hydrophilic region. In the bulk region, $P_{res}(t)$ of PVA decays more slowly than those of PVME and PNiPAM as expected from the volume of the region.

In the calculation of a time correlation function $C(t)$ for water molecules in each region, the molecules which stay in the region from time t_0 to t contribute to $C(t)$ at time t. $C(t)$ is normalized by accumulation numbers, which are proportional to $P_{res}(t)$.

Analysis of Hydrogen-Bond Dynamics. Formation and destruction of hydrogen bonds are recurring in hydrogels. Several definitions of hydrogen-bond time correlations have been developed in different ways.[2,10−13] The mean hydrogen-bond lifetimes, τ_{HB}, somewhat differ depending on the definition.

Rapaport[11] performed an analysis of the hydrogen-bond lifetime using two different kinds of autocorrelation functions: "intermittent" and "continuous" ones. Autocorrelation functions of the form

$$C_x(t) = \frac{\langle \sum_{ij} s_{ij}(t + t_0) \cdot s_{ij}(t_0) \rangle}{\langle \sum_{ij} s_{ij}(t_0) \cdot s_{ij}(t_0) \rangle} \qquad (1)$$

are defined for both kinds of analysis, with the subscript x indicating whether the intermittent (I) or continuous (C) version is intended. In order to study the intermittent lifetime, a quantity $s_{ij}(t)$ is defined for a pair of molecules, i and j, at time t as

$$s_{ij}(t) = \begin{cases} 1 & \text{(bonded)} \\ 0 & \text{(nonbonded)} \end{cases} \qquad (2)$$

Only those pairs of molecules which have $s_{ij} = 1$ at $t = 0$ are included. This type of analysis focused on the elapsed time until the final breakage of the bond occurred. If the same hydrogen-bond pairs persist for a long period, $C_I(t)$ values have a long tail. If exchanges of bond pairs occur frequently, the values of $C_I(t)$

decrease in a short time. The information related to the exchange of hydrogen-bond pairs can be obtained from this analysis. In the analysis of continous lifetime, each $s_{ij}(t)$ is allowed to make just one transition from unity to zero. The elapsed time until the first breakage is observed from this type of analysis. Rapaport showed that the total time scale for $C_I(t)$ is an order of magnitude longer than that of $C_C(t)$.

In the present study, we have performed two types of analyses to elucidate hydrogen-bond dynamics. One is the direct measurement of the distribution of hydrogen-bond lifetime, which is roughly equivalent to the continous lifetime of Rapaport. $P_{on}(t)$ is defined as a distribution of time from formation of a hydrogen bond to destruction of the bond. $P_{off}(t)$ is defined as a distribution of time from destruction of a hydrogen bond to re-formation of the bond which was bonded previously with the exactly same pair. The histograms of $P_{on}(t)$ and $P_{off}(t)$ are smoothed by averaging the values of successive 5 columns. The other analysis is similar to the intermittent time correlation $C_I(t)$ of Rapaport. For water molecules $s_{ij}(t)$ is defined for a pair of molecules i and j. The subscript i (and j) denotes polar groups −OH, −O−, =O, or −NH− for polymers. The sums are taken over the atom pairs which have already formed hydrogen bonds at time t_0 and are averaged over all the time orgins t_0. Calculation is performed for 5000 points of time origins (0.01 ps interval) during 50 ps. Below in our paper, $C_{HB}(t)$ denotes this function.

The average hydrogen-bond lifetime τ_{on} and re-formation time τ_{off} are calculated from $P_{on}(t)$ and $P_{off}(t)$, respectively, as

$$\tau_x = \int_0^\infty t\, P_x(t)\, dt \tag{3}$$

where x denotes "on" or "off." Another time constant τ_{HB} is evaluated from the hydrogen-bond autocorrelation function $C_{HB}(t)$ by defining the exponential decay of $C_{HB}(t)$.

$$C_{HB}(t) \sim \exp\left(-\frac{t}{\tau_{HB}}\right) \tag{4}$$

Rapaport[11] makes it clear that the values of the time constant are highly dependent on the choice of criteria for definition of the hydrogen bond. In his study, the hydrogen bond is defined by the energy criteria. The lifetime varies with the cutoff energy: $V_{HB} = -4$, -3, -2 kcal/mol (-16.7, -12.5, -8.4 kJ/mol). The average hydrogen-bond number also varies from 1.6 to 3.7 by increasing V_{HB} from -4 to -2 kcal/mol. In our study, the hydrogen bond is defined by the geometry definition as described in Part 1. A pair of water molecules are defined to be hydrogen-bonded if distances and an angle satisfy the following conditions:

$$R_{OO} \le 3.60 \text{ Å}$$
$$R_{OH} \le 2.45 \text{ Å} \tag{5}$$
$$\phi \le 30°$$

where R_{OO} and R_{OH} are distances $O_1\cdots O_2$ and $O_1\cdots H_2$ and ϕ is an angle $O_1\cdots O_2-H_2$, where the subscripts 1 and 2 show indices of water molecules. This choice of the distance cutoff is reasonable because it is based on the first minimum of the radial distribution function. Figure 2 shows dependence of average hydrogen-bond number $\langle n_{HB}\rangle$, lifetime τ_{on}, and reformation time τ_{off} on the cutoff angle ϕ for pure water. Although the average number of hydrogen bonds increases with increase of ϕ, $\langle n_{HB}\rangle$ reaches an asymptotic value at $\phi = 30°$, at which hydrogen bonds are cut off in our analysis. It is expected that the dynamic behavior of hydrogen bonds is also saturated with increasing ϕ. As shown in Figure 2, τ_{on} and τ_{off}, which reflect short-time dynamics of hydrogen bonds, are saturated at slightly larger cutoff angle: $\phi \ge 40°$. Figure 3 shows the hydrogen-bond autocorrelation function $C_{HB}(t)$, which reflects long-time dynamics of hydrogen bonds. The decay curve of $C_{HB}(t)$ reaches asymptotic one at $\phi \ge 30°$. Accordingly, equilibrium properties and long-time dynamics of hydrogen bonds are independent of the cutoff angle at $\phi \ge 30°$, while short-time dynamics slightly depends on that.

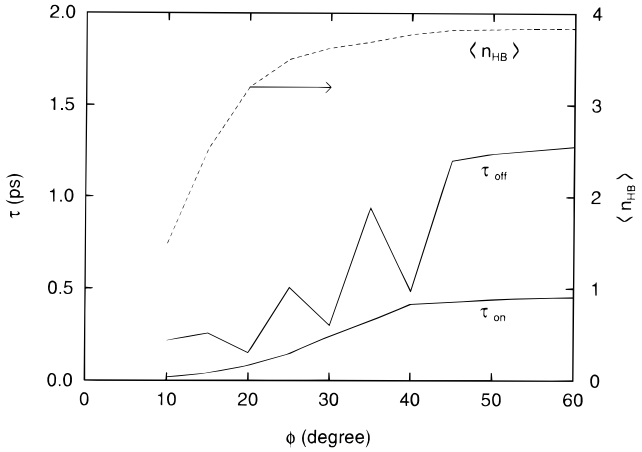

Figure 2. Dependence of average hydrogen-bond number $\langle n_{HB}\rangle$, lifetimes τ_{on}, and re-formation time τ_{off} on the criteria of hydrogen bonds. Dependence on cutoff angle ϕ is plotted for pure water with fixed cutoff lengths $R_{OO} \le 3.60$ Å and $R_{OH} \le 2.45$ Å.

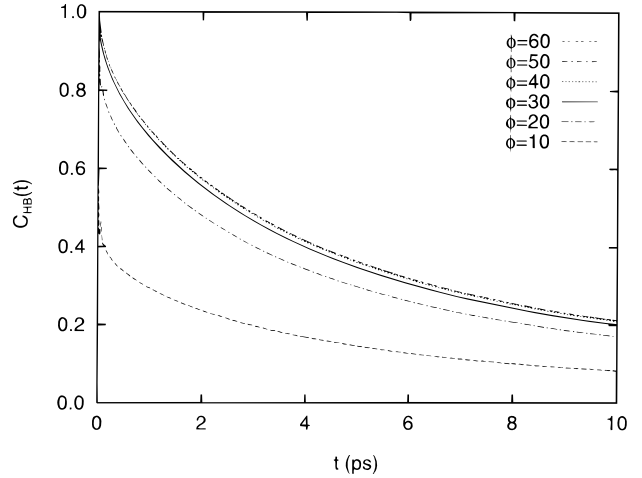

Figure 3. Dependence of the hydrogen-bond autocorrelation function $C_{HB}(t)$ on the cutoff angle ϕ with fixed cutoff lengths $R_{OO} \le 3.60$ Å and $R_{OH} \le 2.45$ Å.

Hydrogen-Bond Dynamics of Polymer. Figures 4a and 4b show distribution of the lifetime $P_{on}(t)$ and that of the re-formation time $P_{off}(t)$, respectively, of hydrogen bonds of polymers in the hydrogel models with $c_w \simeq 50$ wt % at 300 K. The average hydrogen-bond lifetime τ_{on} and re-formation time τ_{off} are tabulated in Table 1. Figure 5 shows the hydrogen-bond autocorrelation function $C_{HB}(t)$ of polymers with $c_w = 50$ wt %. Similar results are obtained for the systems with the other water contents. All the correlations become

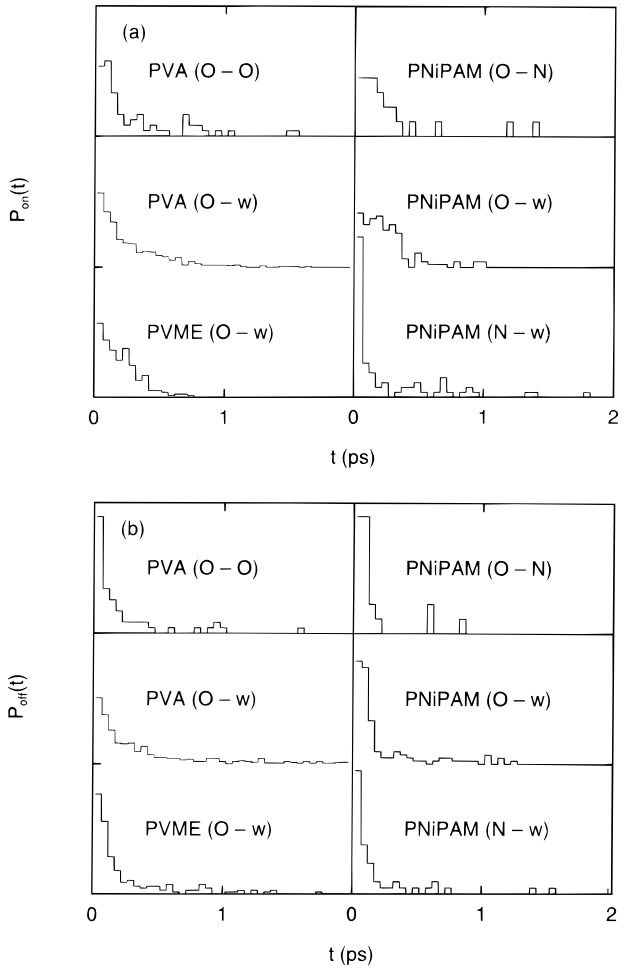

Figure 4. Distributions of (a) lifetime $P_{on}(t)$ and (b) re-formation time $P_{off}(t)$ of hydrogen bonds of polymers in hydrogel models with a water content of 50 wt % at 300 K. Symbols "O" and "N" indicate oxygen and nitrogen atoms of polymers, respectively, and "w" indicates water.

Table 1. Hydrogen-Bond Lifetime of Polymers at 300 K[a]

group	polymer−water	polymer−polymer
	Lifetime τ_{on}	
−OH (PVA)	0.28	0.36
−O− (PVME)	0.18	
−CO− (PNiPAM)	0.23	0.33
−NH− (PNiPAM)	0.52	
	Re-formation Time τ_{off}	
−OH (PVA)	0.76	0.98
−O− (PVME)	0.50	
−CO− (PNiPAM)	0.38	0.72
−NH− (PNiPAM)	1.49	

[a] For hydrogel models with a water content of 50 wt % in units of ps (10^{-12} s).

higher for a longer time, with decreasing the water contents. The relaxation times of $C_{HB}(t)$, τ_{HB}, are listed in Table 2. The fitting of the single exponential function to $C_{HB}(t)$ is a rather rough estimate of τ_{HB} for the present system. The relaxation time varies with a fitting range of t. The results for two different fitting ranges, 2−10 and 1−3 ps, are listed in the table.

For the hydrogen bonds between polar groups of polymers, rapid destruction and re-formation whose time scale is shorter than 0.1 ps are observed dominantly in both $P_{on}(t)$ and $P_{off}(t)$. Very slow processes of the destruction and re-formation are also seen. The lifetimes are longer than that of pure water; 0.23 ps. The initial decay of $C_{HB}(t)$ reflects short-time components of $P_{on}(t)$. $C_{HB}(t)$ does not decay in the long-time region; the relaxation time is very long as listed in Table 2. For PNiPAM, which has large side chains, temperature dependence of $C_{HB}(t)$ is very small. The exchange of hydrogen-bond pair is suppressed because global conformational transition of polymer chains is hard to occur in our simulation.

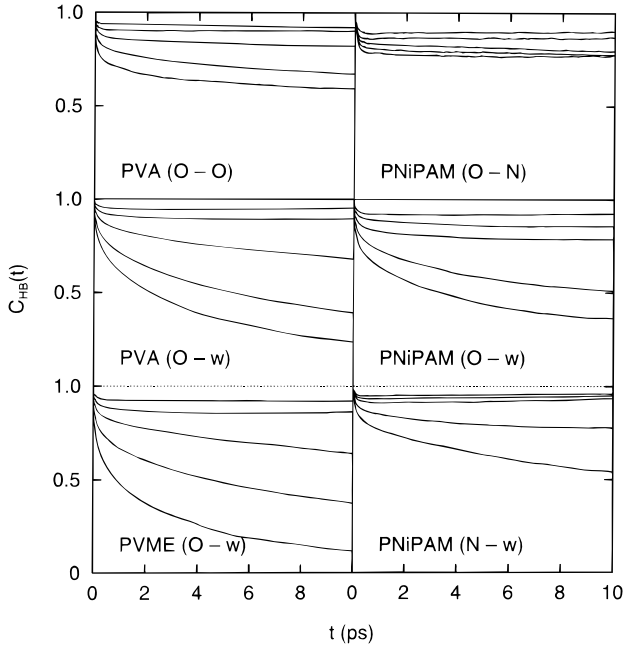

Figure 5. Hydrogen-bond autocorrelation function $C_{HB}(t)$ of polymers in hydrogel models with a water content of 50 wt %. Symbols "O" and "N" indicate oxygen and nitrogen atoms of polymers, respectively, and "w" indicates water. The $C_{HB}(t)$ functions are calculated at 200, 250, 300, 350, and 400 K; each corresponds to the upper to the lower lines in each part.

Table 2. Relaxation Time of Hydrogen-Bond Correlation of Polymers at 300 K[a]

group	polymer−water	polymer−polymer
−OH (PVA)	51 (29)	230 (130)
−O− (PVME)	44 (31)	
−CO− (PNiPAM)	280 (74)	200 (160)
−NH− (PNiPAM)	∞ (∞)	

[a] Obtained from least-squares fitting with a range of 2−10 ps (in parentheses: 1−3 ps) for hydrogel models with a water content of 50 wt % in units of ps (10^{-12} s).

For the hydrogen bonds between water and polymers, the distributions of $P_{on}(t)$ and $P_{off}(t)$ are highly dependent on the species of polar groups. The distributions for −OH of PVA and −O− of PVME are all similar to that for pure water (see Figure 6). Those for PVA have components longer than 1 ps, those for PVME do not. As shown in Part 1,[1] the hydrogen-bond energy is higher for PVME than PVA. This leads to shorter τ_{on} of PVME. For the =O group of PNiPAM, the populations shorter than 0.1 ps are small; the distribution $P_{on}(t)$ broadens toward 0.5 ps. There are few pairs whose hydrogen-bond lifetime is longer than 1 ps. As for −NH− group of PNiPAM, there are some pairs whose lifetime is fairly long as in the case of hydrogen bonds between polar groups of polymers, though the population shorter than 0.05 ps is dominant. The lifetime τ_{on} is very long for this group.

$C_{HB}(t)$ also depends on the characters of polar groups. The polar groups of PVA and PVME show similar decays of $C_{HB}(t)$. Those for PNiPAM exhibit longer correlation of hydrogen-bond pairs, especially for the

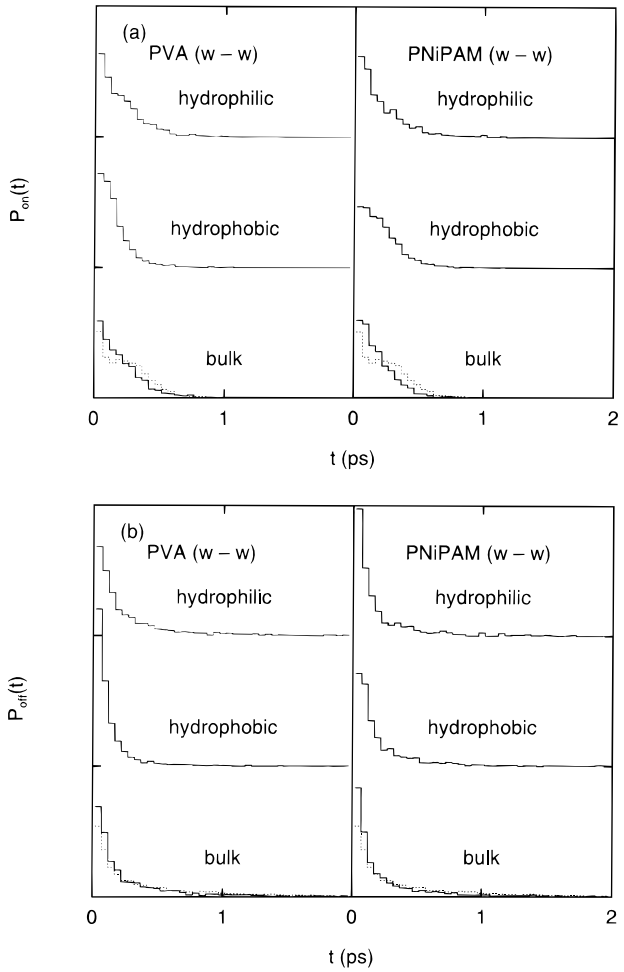

Figure 6. Distributions of (a) lifetime $P_{on}(t)$ and (b) re-formation time $P_{off}(t)$ of water−water hydrogen bonds in hydrogel models with a water content of 50 wt % at 300 K. Dotted lines show those for pure water.

−NH− group. In the hydrophilic region of PNiPAM, the decay of $P_{res}(t)$ of water is slower than that of the other systems, as shown in Figure 1a. The profiles of $C_{HB}(t)$ also show that smaller numbers of exchange of water molecules occur and the hydrogen bonds continue for a long time.

Hydrogen-Bond Dynamics of Water. Figures 6a and 6b show distribution of the lifetime $P_{on}(t)$ and that of the re-formation time $P_{off}(t)$, respectively, of water−water hydrogen bonds in the hydrogel models with $c_w \simeq 50$ wt % at 300 K. The distributions are calculated for three regions classified above. Interregional bonds are defined to contribute to the statistics of both spatial regions. Figure 7 shows $C_{HB}(t)$. Time constants of relaxation are tabulated in Table 3 and 4.

In the bulk region the distributions resemble that in pure water. The distributions around polymers are different from those in pure water. In the hydrophobic region, the lifetime of PNiPAM is shifted to longer time than that of PVA. In estimation of τ_{on} and τ_{off} listed in Table 3 the classification raises some problems. All the lifetimes and re-formation times for classified regions are shorter than those for nonclassified one. This is an artifact caused by classification. Because the residence rate $P_{res}(t)$ of water rapidly decays at short-time region, contribution to the distribution of $P_{on}(t)$ and $P_{off}(t)$ at longer time is partly excluded from statistics. Concerning the nonclassified region, the lifetimes in hydrogels are slightly longer than that in pure water.

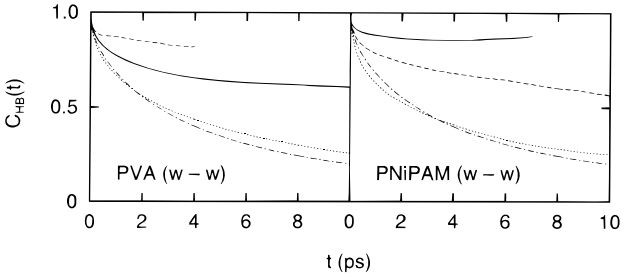

Figure 7. Hydrogen-bond autocorrelation function $C_{HB}(t)$ of water in hydrogel models with a water content of 50 wt % at 300 K: (solid line) hydrophilic region, (dashed line) hydrophobic region, (dotted line) bulk region, and (dash-dot line) pure water.

Table 3. Hydrogen-Bond Lifetime of Water at 300 K[a]

polymer	hydrophilic	hydrophobic	bulk	nonclassified
		Lifetime τ_{on}		
PVA	0.19	0.13	0.19	0.25
PVME	0.20	0.21	0.16	0.26
PNiPAM	0.21	0.19	0.17	0.25
pure water				0.23
		Re-formation Time τ_{off}		
PVA	0.36	0.12	0.49	0.87
PVME	0.23	0.34	0.37	0.81
PNiPAM	0.25	0.28	0.38	0.79
pure water				0.71

[a] See footnote of Table 1.

Table 4. Relaxation Time of Hydrogen-Bond Correlation of Water at 300 K[a]

polymer	hydrophilic	hydrophobic	bulk
PVA	60 (16)	∞ (42)	11 (6.5)
PVME	120 (35)	38 (21)	11 (6.8)
PNiPAM	∞ (71)	32 (19)	11 (6.7)
pure water			8.0 (5.4)

[a] See footnote of Table 2.

The re-formation times are longer than that in pure water. Correlation of hydrogen-bonded pair is stronger in hydrogels. This is reflected on the decay curve of $C_{HB}(t)$.

The decay of $C_{HB}(t)$ in the bulk region is almost the same as that in pure water; the relaxation time in the former is slightly longer. The decay in the hydrophilic and hydrophobic regions is much slower. The results for PVA are shown in the left part of Figure 7. In the hydrophilic region, rearrangements of water−water hydrogen bonds are suppressed because of the decrease in the mobility of water molecules by polymer−water hydrogen bonds. In the hydrophobic region, the correlation for a long time cannot be calculated for PVA since $P_{res}(t)$ decays fast. The results for PNiPAM are shown in the right part of Figure 7. Since the exchanges of water molecules are hard to occur as described previously, only a small number of rearrangements is observed for water−water hydrogen bonds in the hydrophilic region. The correlation in the hydrophobic region is also higher than that in the bulk region.

Similar results are obtained for the systems with the other water contents. All the correlations become higher for a longer time, with decreasing the water contents, for both polymer−water and water−water hydrogen bonds. This is because the diffusivity of water molecules decreases in the systems with low water contents.

Diffusion of Water. To examine the effects of polymers on the translational motions of water, the

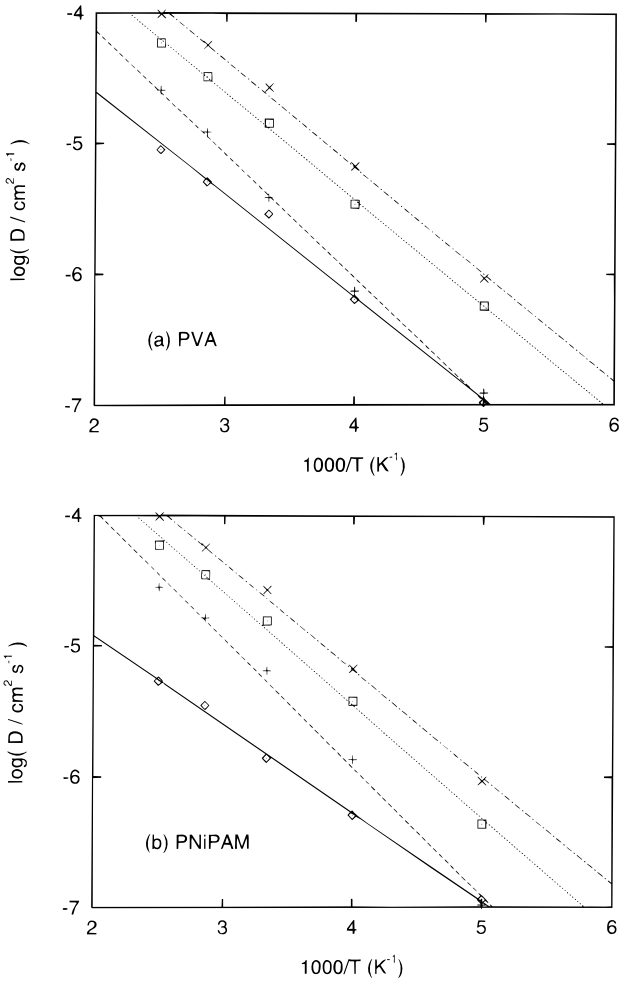

Figure 8. Arrhenius plot of diffusion coefficient D of water for (a) PVA and (b) PNiPAM hydrogel models with a water content of 50 wt %: (solid line) hydrophilic region, (dashed line) hydrophobic region, (dotted line) bulk region, and (dash-dot line) pure water. The straight lines show the least-squares fits.

diffusion coefficient of water is calculated for three regions classified above. The diffusion coefficient D is calculated from the mean-square displacement (MSD) as

$$D = \lim_{t\to\infty} \frac{1}{6t}\langle[\mathbf{R}(t + t_0) - \mathbf{R}(t_0)]^2\rangle \qquad (6)$$

where $\mathbf{R}(t)$ is the center of mass of a water molecule at time t and $\langle ... \rangle$ means the ensemble average.

The MSD's deviated from linear at long time scales, when those are calculated for classified regions. This is because the relaxation of $P_{res}(t)$ is very fast in the hydrophilic region of PVME and the hydrophobic region of the three polymers, and the number of samples becomes very small in the regions. The long-time behavior is characterized only by the particular samples which stay in the region for a long period. The molecules staying in a specific region for a long time have low mobility, which gives rise to the deviation of MSD from a linear line. We should not consider the longer time behavior too seriously for calculation of diffusion coefficients and orientational relaxation time. In the time scales of 0.5−5 ps, the MSD's are approximately linear in time for all the systems. Therefore, the values of D are determined from the least-squares fit with a fitting range of this time scale. Figure 8 shows the Arrhenius plots of D calculated for the systems with $c_w \simeq 50$ wt %. Parts a and b of Figure 8 show the results for PVA and PNiPAM, respectively. The straight lines in the figure are obtained by the least-squares method. The diffusion coefficients are well-fitted to the equation

$$D = D_0 \exp\left(-\frac{E_D}{RT}\right) \qquad (7)$$

from which the activation energy of diffusion, E_D, is calculated.

The experimental[14] diffusion coefficient for pure water is $(2.11-2.66) \times 10^{-5}$ cm^2/s at 298 K. The calculated value at 300 K agrees with the experiments. The calculated value of E_D is 3.7 kcal/mol, which agrees with the experimental values 4.4−4.8 kcal/mol, though slightly smaller.

In the hydrophilic and hydrophobic regions, the motions of water molecules are highly hindered by the presence of polymer chains. The diffusion coefficients are approximately 10−40% of those in pure water. The motions are suppressed more significantly in the hydrophilic region than in the hydrophobic region. For the PVME hydrogel models the motions are also suppressed more significantly in the former region. In the hydrophilic region, the motions are hindered because of tight hydrogen bonds between water and polymers and stabilization of water−water hydrogen bonds. In the hydrophobic region, the motions are hindered because of the structuralization of water. Using MD simulation, Kitao et al.[15] studied the hydration of melittin, which is a bioactive polypeptide consisting of 26 amino acid residues and is a main component of bee venom. The diffusion coefficients of water are calculated in the classified areas around charged, polar, and nonpolar groups and in bulk. The water molecules in the first hydration shell around charged groups are immobilized by the strong interaction. The diffusion coefficients in the first hydration shell around polar and nonpolar groups are 40−50% of that in pure water. These values are the same order as our results.

Even in the bulk region, where water molecules are distant from polymers, D is influenced by polymer and becomes smaller than that in pure water. For the systems with a water content 75 wt %, D values in the bulk region are almost the same as those in pure water. For the systems with lower water contents, however, D values decrease in the bulk region by the presence of polymers. The reason for this is discussed below.

Local Motion of Water. In order to obtain information about the local motion of water molecules, the spectral densities are calculated for the translational motion of water. The spectral density $G(\omega)$ is obtained from the Fourier transform of the translational velocity autocorrelation function as

$$G(\omega) = \frac{2}{\pi}\int_0^\infty \langle \mathbf{v}(t + t_0)\cdot\mathbf{v}(t_0)\rangle \cos(\omega t)\, dt \qquad (8)$$

where $\mathbf{v}(t)$ is the velocity of center of mass of a water molecule at time t, ω is the angular frequency, and $\langle ... \rangle$ means the ensemble average. The spectra are smoothed with a help of a window function.

Figure 9 shows those spectra. The abscissa is wavenumber κ in cm^{-1} and the ordinate is the spectral density $G(\kappa)$ in arbitrary units. In the bulk region, the distributions are almost the same as those in pure water except for the diffusional component near $\kappa = 0$. In the hydrophobic region, the distributions are shifted by 15

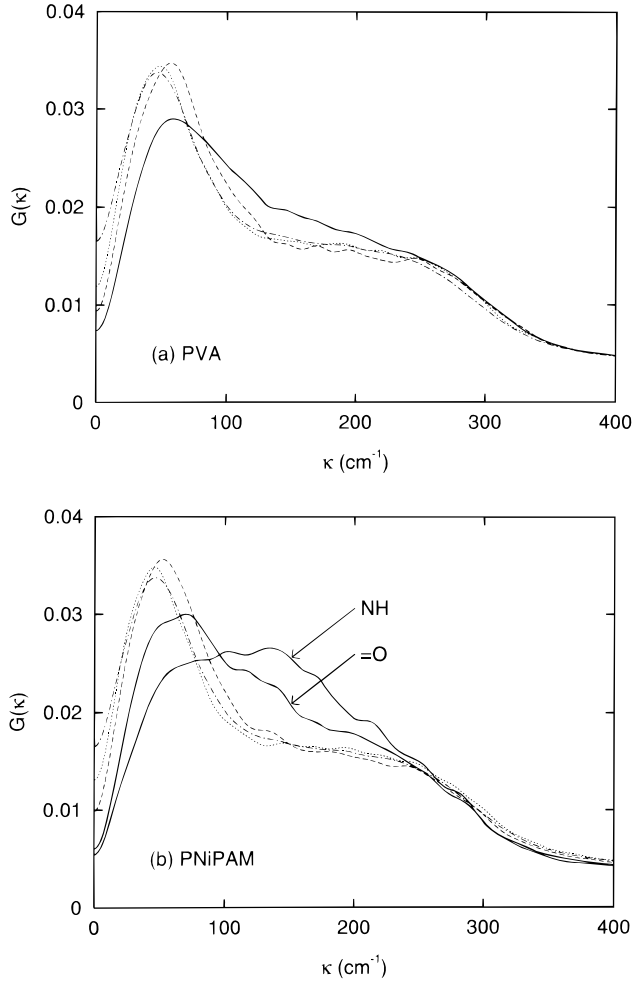

Figure 9. Spectral density $G(\kappa)$ of translational motion of water for (a) PVA and (b) PNiPAM hydrogel models with a water content of 50 wt %: (solid line) hydrophilic region, (dashed line) hydrophobic region, (dotted line) bulk region, and (dash-dot line) pure water.

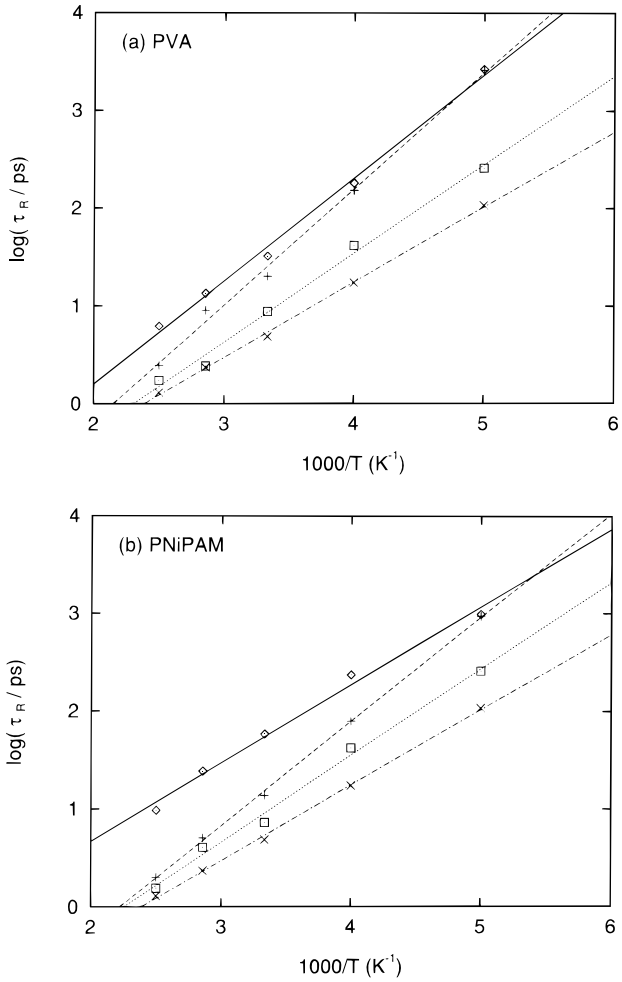

Figure 10. Arrhenius plot of orientational relaxation time τ_R of water for (a) PVA and (b) PNiPAM hydrogel models with a water content of 50 wt %: (solid line) hydrophilic region, (dashed line) hydrophobic region, (dotted line) bulk region, and (dash-dot line) pure water. The straight lines show the least-squares fits.

cm^{-1} toward high frequency without deformation of the waveform. It is evident that the structure enhancement gives rise to this shift. There is little difference between PVA and PNiPAM. In the hydrophilic region, the intensity curves are highly deformed by the polymers; the high frequency components of 100−250 cm^{-1} increase. The intensities of the high frequency components follow the order of

$$\text{NH(PNiPAM)} > \text{CO(PNiPAM)} > \text{OH(PVA)}$$

These results together with the analyses of the lifetime of hydrogen bonds lead us to a picture that water molecules around the −NH− groups are strongly bound to the groups and are also making intermittent formation and destruction of hydrogen bonds in a short time scale.

Orientational Relaxation of Water. The effect of polymers on the rotational motions of water is examined using the orientational time correlation functions[2]

$$C_l^{\mathrm{R}}(t) = \langle P_l[\mathbf{u}(t_0)\cdot\mathbf{u}(t + t_0)]\rangle \tag{9}$$

where $P_l(x)$ is the lth order Legendre polynomial and $\mathbf{u}(t)$ is a vector embedded in the molecule at time t. In the present study, $\mathbf{u}(t)$ is along the dipole vector of water molecules. In the time region shorter than 0.1 ps, the rapid relaxation caused by the libration of molecules is observed in $C_l^{\mathrm{R}}(t)$. In the time regions longer than 0.5 ps, the single exponential decay is observed. The orientational relaxation time τ_R is calculated by fitting the decay of $C_l^{\mathrm{R}}(t)$ to the exponential function.

$$C_l^{\mathrm{R}}(t) \sim \exp\left(-\frac{t}{\tau_{\mathrm{R}}}\right) \tag{10}$$

When water molecules are classified into the regions, the decay of $C_l^{\mathrm{R}}(t)$ deviates from a single exponential function because of the problems previously described. In this case, the fitting procedure is performed with supplementing the long time scale behavior.

Figure 10 shows the Arrhenius plots of τ_R for water in each region of hydrogel models with a water content 50 wt %. Parts a and b of Figure 10 show those for PVA and PNiPAM, respectively. The plots are linear in all the regions. In the hydrophilic and hydrophobic regions, also the rotational motions of water molecules are highly suppressed by the presence of polymer chains. The motions are suppressed more severely in the hydrophilic region than in the hydrophobic region. The values of τ_R are large around the hydrophilic groups because the motion of water molecules is constrained by the water−polymer hydrogen bonds. The values of τ_R are also large around the hydrophobic groups because the structure of water is promoted in the hydrophobic region.

Even in the bulk region, which is far from polymers, τ_R is influenced by polymer and is longer than that in pure water. Although τ_R values in the bulk region are not affected by the polymers for the systems with a water content 75 wt %, the values decrease for the systems with lower water contents. In the bulk region, hydrogen-bond numbers and local motions are equal to those in pure water, irrespective of water contents. The translational diffusion and the orientational relaxation of water molecules are, however, suppressed by polymers for the systems of lower water contents. Water molecules are continuously spread over in whole the simulation cell and are preferentially dissolved in the bulk region for the system with a high water content. On the other hand, water molecules are compartmentalized for the system with a low water content. Therefore, though the local structure and local motion of water are not affected, the mobility of long time scales is suppressed in the latter system.

Comparison with Hydration in Other Systems. Hydration of small molecules has been studied through computer simulation as reviewed by several authors.[2,16,17] Rossky and Karplus[18] studied structure and dynamics of the hydration shell for alanine dipeptide through MD simulation. The translational and rotational mobility of water molecules is highly suppressed around hydrophobic groups, while slightly suppressed around hydrophilic ones. Tanaka et al. performed MD simulations for aqueous solutions of *tert*-butyl alcohol (TBA)[19] and that of urea.[20] In spite of strong interaction between water and urea, the diffusion coefficient of water is less suppressed in the urea solution than in TBA solution. In the vicinity of apolar molecules, water becomes more structured and less mobile by so-called hydrophobic effects.[21,22] In the present study, mobility of water is significantly lowered around both hydrophilic and hydrophobic groups. Hydrophobic effects play an important role also in hydrogels. Water molecules in hydrogels are strongly bound to hydrophilic groups of polymer chains, which relax very slowly compared with small molecules. This leads to different behavior of water around hydrophilic groups in hydrogels from that around small molecules.

The slow relaxation of a solute is the same situation as in the case of hydration of proteins. In the hydration shell of melittin, which is a bioactive polypeptide consisting of 26 amino acid residues, mobility of water is significantly suppressed around charged, polar, and nonpolar groups of the protein.[15] The water molecules in the first hydration shell of a charged group are immobilized by the strong interaction with the group. In the hydration of proteins, water molecules are bound to the surface area of protein of rather compact conformation. On the other hand, water molecules are surrounded by polymer networks in hydrogels. Large hydrophobic side chains impose a constraint on the mutual orientation of water and polar group. Finite size of the local solvent droplet reduces the mobility of water molecules even in the bulk region of our system.

Conclusion

MD simulations have been carried out for the hydrogel models of PVA, PVME, and PNiPAM to elucidate the structure and dynamics between water and polymers. The simulations are performed for the systems with water contents 0, 25, 50, and 75 wt % at five temperatures ranging from 200 to 400 K. The dynamics of hydrogen bonds in the hydrogels is investigated through the lifetime distribution and the hydrogen-bond correlation function. The translational diffusion and the orientational relaxation are analyzed for water molecules which are classified into three categories: (1) around hydrophilic groups, (2) around hydrophobic groups, and (3) the remaining bulk region.

The effects of polymers on the properties of water molecules are varied with the species of polar groups. The characters of the hydrophilic groups are reflected in the lifetime of hydrogen bonds, the spectral density, etc. Around the −NH− groups of PNiPAM, the analyses such as the residence rate, the lifetime of hydrogen bonds, and the hydrogen-bond autocorrelation function show that exchange of water molecules hardly occurs and the polymer−water hydrogen bonds persist for a long period. Although water molecules are strongly bound to the −NH− groups, the populations having a lifetime of hydrogen bonds shorter than 0.05 ps are dominant in the lifetime distribution. Those of very long time scales are also observed. This implies that the formation and destruction of hydrogen bonds are recurring in a short time scale. This is consistent with what we observed in the translational spectral density.

The mobility of water molecules is highly reduced around polymer chains for both translational and rotational motions. The mobility is reduced because of the hydrogen bonds between water and polymers around the hydrophilic groups and because of the structuralization of water around the hydrophobic groups. In the bulk region, the hydrogen-bond numbers and local motions are equal to those in pure water irrespective of water contents. The mobility of long time scales is, however, lowered by polymers for the systems with low water contents. Compartmentation of water is one of the reasons.

In this paper, several analyses are made to elucidate interplay between water and polymers, with attention directed mainly to the properties of water molecules. The effect of water molecules on the local motions of polymers is also an interesting subject. A discontinuous change is expected in the temperature dependence of mobility of water molecules around the phase transition temperature.[23] In this study, however, it could not be observed partly because the simulation time is not long enough to observe the phase transition. Longer time scale simulations or more macroscopic models are needed since the entropy terms of polymer chains should be considered to describe the volume phase transition phenomena. The functional separation membrane is one of the applications of hydrogels. Cooperative motions of water and polymers play an important role in the permeation phenomenon of gases in hydrogels. Further studies should be carried out to elucidate these phenomena.

Acknowledgment. Generous amounts of computer time were provided by the Computer Center, Institute for Molecular Science. Computer time was also provided by the Supercomputer Laboratory, Institute for Chemical Research, Kyoto University.

References and Notes

(1) Tamai, Y.; Tanaka, H.; Nakanishi, K. *Macromolecules* **1996**, *29*, 6750−6760.
(2) Ladanyi, B. M.; Skaf, M. S. *Annu. Rev. Phys. Chem.* **1993**, *44*, 335−368.
(3) Ohmine, I.; Tanaka, H. *Chem. Rev.* **1993**, *93*, 2545−2566.
(4) Nosé, S. *J. Chem. Phys.* **1984**, *81*, 511−519.
(5) Andersen, H. C. *J. Chem. Phys.* **1980**, *72*, 2384−2393.

(6) Jorgensen, W. L.; Tirado-Rives, J. *J. Am. Chem. Soc.* **1988**, *110*, 1657−1666.
(7) Berendsen, H. J. C.; Grigera, J. R.; Straatsma, T. P. *J. Phys. Chem.* **1987**, *91*, 6269−6271.
(8) Allen, M. P.; Tildesley, D. J. *Computer Simulation of Liquids*; Oxford University Press: Oxford, U.K. , 1987; pp 156−162.
(9) Ryckaert, J. P.; Ciccotti, G.; Berendsen, H. J. C. *J. Comput. Phys.* **1977**, *23*, 327−341.
(10) Stillinger, F. H. *Adv. Chem. Phys.* **1975**, *31*, 1−101.
(11) Rapaport, D. C. *Mol. Phys.* **1983**, *50*, 1151−1162.
(12) Matsumoto, M.; Gubbins, K. E. *J. Chem. Phys.* **1990**, *93*, 1981−1994.
(13) Luzar, A.; Chandler, D. *J. Chem. Phys.* **1993**, *98*, 8160−8173.
(14) Eisenberg, D.; Kauzmann, W. *The Structure and Properties of Water*; Oxford Univeristy Press: London, U.K., 1969.
(15) Kitao, A.; Hirata, F.; Gō, N. *J. Phys. Chem.* **1993**, *97*, 10223−10230.
(16) Rossky, P. J. *Annu. Rev. Phys. Chem.* **1985**, *36*, 321−346.
(17) Pratt, L. R. *Annu. Rev. Phys. Chem.* **1985**, *36*, 433−449.
(18) Rossky, P. J.; Karplus, M. *J. Am. Chem. Soc.* **1979**, *101*, 1913−1937.
(19) Tanaka, H.; Nakanishi, K.; Touhara, H. *J. Chem. Phys.* **1984**, *81*, 4065.
(20) Tanaka, H.; Nakanishi, K.; Touhara, H. *J. Chem. Phys.* **1985**, *82*, 5184−5191.
(21) Franks, F., Ed. *Water, A Comprehensive Treatise*; Plenum Press: New York, 1975; Vol. 4.
(22) Ben-Naim, A. *Hydrophobic Interactions*; Plenum Press: New York, 1980.
(23) Ohta, H.; Ando, I.; Fujishige, S.; Kubota, K. *J. Polym. Sci., Polym. Phys. Ed.* **1991**, *29*, 963−968.

MA960961R